Experimental study of mixing of density-stratified fluid in a cylindrical tank by a diagonal jet

Conference Paper

Author(s):
Degawa, T.; Uno, K.; Uchiyama, T.

Publication date:
2018-10-05

Permanent link:
https://doi.org/10.3929/ethz-b-000279236

EXPERIMENTAL STUDY OF MIXING OF DENSITY-STRATIFIED FLUID IN A CYLINDRICAL TANK BY A DIAGONAL JET

T. Degawa[1,c], K. Uno[2], T. Uchiyama[1]

[1]Institute of Materials and Systems for Sustainability, Nagoya University, Nagoya 464-8603, Japan
[2] Nippon Steel & Sumitomo Metal Corporation, Tokyo 100-8071, Japan
[c]Corresponding author: Tel.: +81527894219; Fax: +81527894219; Email: degawa@imass.nagoya-u.ac.jp

KEYWORDS:
Main subjects: mixing, flow visualization, concentration measurement
Fluid: jet, density-stratified fluid
Visualization method(s): Planar Laser Induced Fluorescence, Particle Image Velocimetry
Other keywords: cylindrical tank, density interface, free surface

ABSTRACT: *This study experimentally investigates the mixing of two-layer density-stratified fluid in a cylindrical tank by a diagonal jet. The upper and lower fluids are water and an aqueous solution of sodium chloride (NaCl), respectively, and the lower fluid issues from a nozzle on the tank bottom. The angle between the jet centerline and the tank bottom is 60°, and the mass concentration of the NaCl solution is 0.02. The mixing in cases that the Reynolds numbers of the jets are 713, 2319, and 3565 are investigated. The velocity fields in the central vertical cross-section are measured with a PIV system by tracing nylon particles with the diameter of 80 μm. The concentration fields in the section are visualized using Rhodamine B as the fluorescent dye. They are also measured using PLIF from visualized images and the progresses of the mixing are evaluated quantitatively. The investigation clarifies the relationship between the mixing phenomena and the Reynolds number of the jet.*

1 Introduction

Liquefied natural gas (LNG) has attracted considerable attention because of its low environmental load. It is important for Japan to sustain stable energy supply and to store energy resources since most energy resources rely on imports. For the efficient storage of imported LNG, many kinds of LNG from different production areas are stored in the same LNG tank. As the density of LNG is specific to the production areas and purification plants, density stratification sometimes occur in the tank. The density of such stratified LNG changes owing to heat input from outside of the tank, for instance sunlight and geothermal heat. When the density of the lower LNG layer becomes lower than that of the upper layer, sudden mixing, known as rollover, occurs. The rollover generates large amounts of vaporized gases, which cause severe damage of the storage tank. Thus, the prevention and elimination of the LNG stratification are essential for the operation of LNG storage tanks.

Mixing phenomena of density-stratified fluids in tanks have been studied via laboratory-based experiments. Mixing induced by a jet issuing from a nozzle mounted on the top or bottom of the tank has been investigated [1]-[4]. Mixing LNG by a jet issuing from a nozzle on the bottom of the tank is considered to be a promising technique for preventing and eliminating stratification in LNG storage tanks. The authors performed experiments to investigate mixing phenomena by a jet issuing into a two-layer density-stratified fluid in a rectangular [5] and cylindrical tank [6]. The upper and lower fluids were water and an aqueous solution of sodium chloride (NaCl), respectively, and the lower fluid was issued vertically and diagonally upward from a nozzle on the bottom of the tank. The authors also conducted numerical simulations [7][8] under the same condition as the authors' previous experiments [5][6] and successfully complemented those experimental investigations.

In this study, laboratory experiments are conducted for quantitative investigation of mixing phenomena by a jet issuing into a two-layer density-stratified fluid in a cylindrical tank. The velocity and concentration fields in the central vertical cross-section passing through the jet centerline are measured using the Particle Imaging Velocimetry (PIV) and the Planer Laser Induced Fluorescence (PLIF) [9], respectively.

2 Experimental Condition

2.1 Experimental Setup

A schematic of the experimental setup is shown in Fig. 1. The tank is made of transparent acrylic resin to enable visualization of the fluids. The diameter and height are 295 mm and 250 mm, respectively. A nozzle is mounted on the tank bottom near the side wall of the tank. The origin of the coordinates is set at the center of a horizontal plain passing through the nozzle outlet. The x-y plane is horizontal and z-axis is vertical. The horizontal direction of jet is along x-axis. The inner diameter of the nozzle d is 10 mm, and angle between the centerline of the nozzle and the x-axis is 60 deg. The nozzle outlet is positioned 45 mm away from the tank wall and $6d$ above the tank bottom. The nozzle is connected to a circular hole on the tank bottom via a tube, and a pump and a flowmeter are installed between the hole and nozzle.

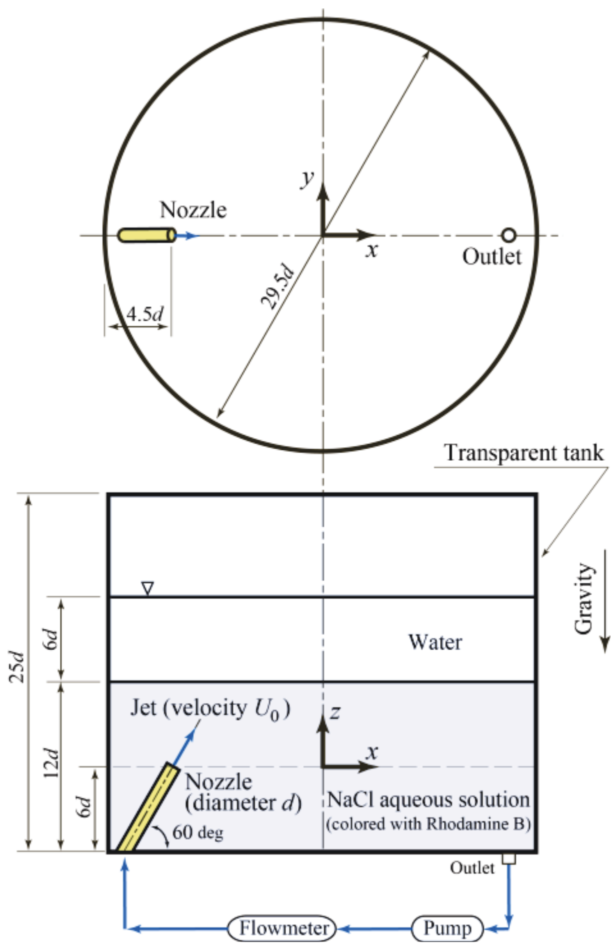

Fig. 1 Experimental Set-up

Initially ($t = 0$), a two-layer density-stratified fluid is in a static condition in the tank. The upper and lower fluids are water and an aqueous solution of NaCl, respectively. The vertical thicknesses of the upper and lower fluids are $6d$ and $12d$, respectively. The mass concentration of the aqueous solution of NaCl is 0.02.

2.2 Experimental Method

At a time $t > 0$, the lower fluid (aqueous solution of NaCl) issues from the nozzle. The mean velocity in the nozzle outlet section denoted by U_0 is calculated from mass flowrate. The volume of the fluids in the tank is maintained at a constant level using pump-driven fluid circulation.

The water velocity in the central vertical cross-section (x-z section) is measured with a particle image velocimetry (PIV) system by treating nylon particles (mean diameter: 80 μm, specific weight: 1.02) added to upper and lower fluids. Images of the section are captured by a video camera using a laser light sheet (power: 1 W, wavelength: 532 nm, thickness: 1 mm). The laser light sheet is irradiated from the bottom of the tank. The framerate of the camera is 200 fps. To visualize the flows in the central vertical cross-section, a small amount of fluorescent dye (Rhodamine B) is uniformly added to the lower fluid. The fluorescence of the dye is captured using another video camera. The framerates of the camera is 30 fps. The concentrations are measured using PLIF [9] from the visualized images and progresses of mixing are quantitatively evaluated. The Reynolds number Re is defined as $U_0\, d/\nu$, where ν is the kinetic viscosity of water. The experiments are conducted at $475 \leq \text{Re} \leq 4753$ in a duration of the non-dimensional time t^* ($= td/U_0$) from 0 to 1400.

3 Results

3.1 Jet Behavior

Temporal variations of the jet height are observed using visualized images for every Reynolds numbers. The jet behavior is classified into three patterns, namely A, B, and C, according to the Re value.

Pattern A: The jet reaches the interface without penetrating it but spreads almost horizontally outward along the interface.

Pattern B: The jet penetrates the interface but does not reach the upper water surface. The top of the jet falls back to the interface and spreads horizontally without penetrating the interface again.

Pattern C: The jet reaches the upper water surface, spreads along the surface, and falls back to the interface.

Table 1 lists the patterns of jet behavior (Patterns A, B, and C) for different Re values at $t^* = 500$. Fig. 2 shows visualized images for Re = 713, 2139, and 3565, which represent Pattern A, B, and C, respectively. At Re = 713, local deformation of the density interface caused by the jet reaching the interface is visualized. At Re = 2139, the decline of the jet penetrating the density interface is visualized. The jet deformed the interface and gave rise to mixing along the interface. At Re = 3565, spreading of the jet along the upper surface and active mixing between the jet and the ambient fluid are visualized.

In this study, the Reynolds numbers of 713, 2139, and 3565 are chosen as the representative Reynolds numbers for each pattern, and the velocity and concentration fields at Re = 713, 2139, and 3565 are measured using PIV and PLIF, respectively.

Table 1 Classification of jet behavior

Re	475	713	951	1188	1426	1663	2139	2376	2614	2852	3089	3565	4753

Pattern	A	A	B	B	B	B	B	B	B	B	C	C	C

(a) Re=713 (b) Re=2139 (c) Re=3565

Fig. 2 Visualized flow pattern at Re = 713, 2139, and 3565 in the central vertical cross-section (y=0)

3.2 Temporal Variation of Velocity and Concentration Distribution

Figs. 3, 4, and 5 show the distributions of the time-averaged velocity in the central vertical cross-section passing through the jet centerline (y=0) at Re = 713, 2139, and 3565, respectively. In each figure, the velocities averaged at earlier stage (from t^*=200 to 600), intermediate stage (from t^*=600 to 1000), and later stage (t^*=1000 to 1400) are shown, and the nozzle outlet and initial position of the density interface are indicated by a black dot and a white dashed line, respectively.
Fig. 3 shows the results at Re = 713, the jet behavior is classified as Pattern A. The jet reaches the density interface and spreads almost horizontally along the interface. The velocity slightly spreads in the vertical (z) direction as the horizontal component of the velocity gradually decreases with the lapse of time.
Fig. 4 shows the results at Re = 2139, the jet behavior is classified as Pattern B. The top of the jet penetrates the density interface and falls back to the interface owing to the gravitational effect, as the density of the jet is higher than that of the upper fluid. The fluid descending from the top of the jet spreads horizontally when it again reaches the density interface. This downward flow causes the interface to heave and leads to mixing of the fluids in the lower region along the interface. According to the time-averaged distribution, the downward flow reaches near $z/d = 3$ in the lower layer, the mixing in the lower fluid between jet and ambient fluid occurs at $z/d \geq 3$. The jet height becomes higher over time. At later stage (t^*=1000-1400), the position where the jet falls back to the density interface move outward, namely toward the tank wall on the opposite side of the nozzle. The downward velocity becomes weaker because the spreading of the jet in the upper layer becomes relatively wider.
Fig. 5 shows the results at Re = 3565, the jet behavior is classified as Pattern C. The jet reaches the upper water surface and spreads horizontally just below the water surface. This spreading leads to the weakening of the downward flow which is the cause of the interface heaving. The spreading of the jet along the water surface becomes wider over time, the downward flow is eventually no longer observed.

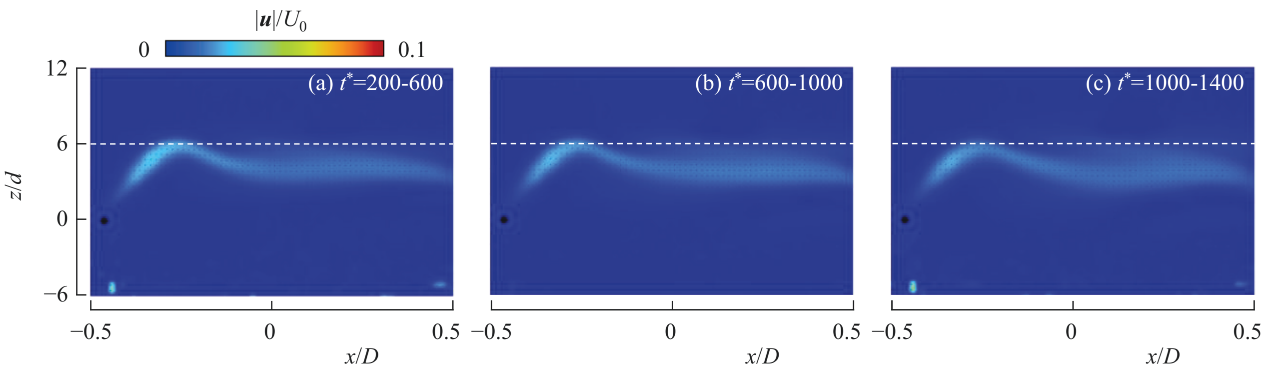

Fig. 3 Time-averaged velocity distribution in the central vertical cross-section of the tank at Re=713

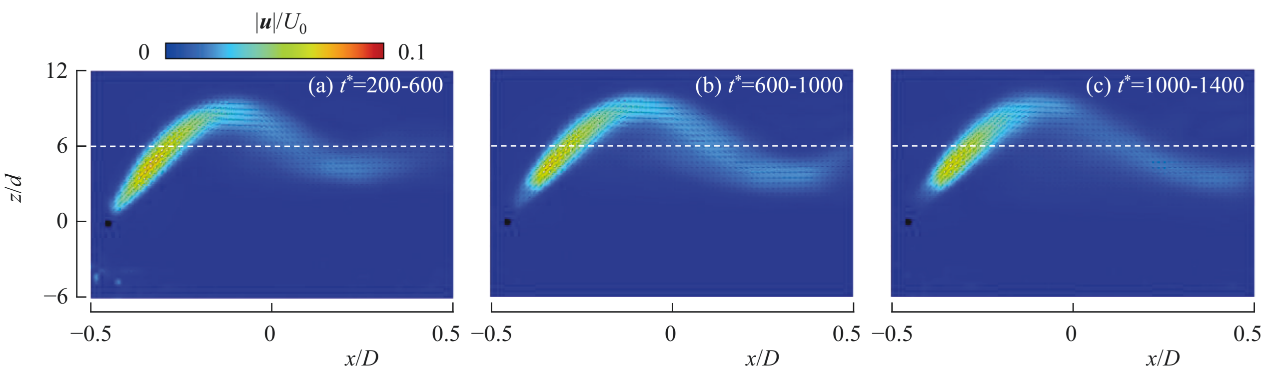

Fig. 4 Time-averaged velocity distribution in the central vertical cross-section of the tank at Re=2139

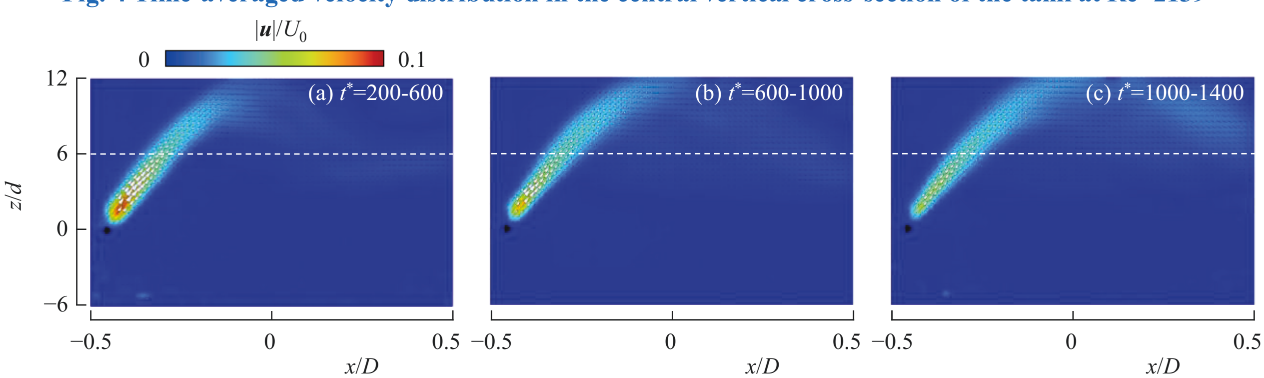

Fig. 5 Time-averaged velocity distribution in the central vertical cross-section of the tank at Re=3565

The concentration C is measured using PLIF in the central vertical cross-section passing through the jet centerline at Re = 713, 2139, and 3565. The time-averaged concentrations $\overline{C}$ from t^*=200 to 600, from t^*=600 to 1000, and from t^*=1000 to 1400 are then calculated. The distributions are shown in Figs. 6, 7, and 8.

Fig. 6 shows the distributions of $\overline{C}$ at Re=713 for Pattern A. The jet reaches the density interface without penetrating it. The jet pushes the interface up locally. In the vicinity of this location, the concentration decreases slightly because the downward flow entrains the upper fluid. The change in concentration within the interface is not remarkable. The mixing gently proceeds near the interface because of the horizontal flow just below the interface with lapse of time. A slight decrement in the concentration due to the mixing is confirmed near the interface at $x/D \geq 0$.

Fig. 7 shows the distributions at Re = 2139 for Pattern B. The jet penetrates the interface but does not reach the water surface. The penetration through the interface is confirmed by the concentration distribution, and the concentration locally increases in the upper layer. The lower fluid transported to the upper layer descends from the top of jet and spreads horizontally, forming an arc-like shape. The downward flow deforms the interface. The layer of mixed fluid vertically spreads above and below the initial position of the interface ($z/d = 6d$). Mixing proceeds mainly in this layer, called the intermediate density layer. The layer is not observed at Re=713. As time passes, the jet height becomes higher and the intermediate density layer thickens.
The concentration distributions at Re=3565 for Pattern C are shown in Fig. 8. The jet reaches the water surface and widely spreads in horizontal direction along the water surface. This spreading of the jet becomes wider over time, as confirmed from the velocity distribution in Fig. 5. Active mixing between the jet and the ambient fluid occurs in the upper layer. The intermediate density layer is thinner than that at Re=2139 because the downward velocity of the lower fluids transported by the jet becomes weaker owing to the horizontal spreading, and the heaving of interface also becomes weaker. At Re=713 and 2139, the mixing is generated by the heaving of interface caused by the horizontal flow owing to the collision between the jet and the density interface. At Re=3565, the mixing at earlier stage proceeds due to the diffusion of lower fluid, which is transported by the jet, in the upper layer and the heaving of the interface by the downward flow. The mixing at later stage mainly proceeds by the diffusion of lower fluid in the upper layer.

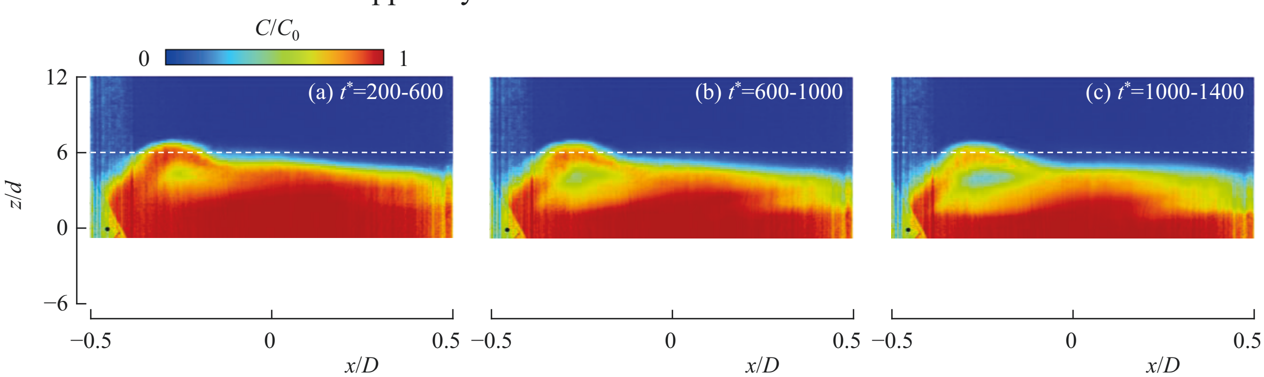

Fig. 6 Time-averaged concentration distribution in the central vertical cross-section of the tank at Re=713

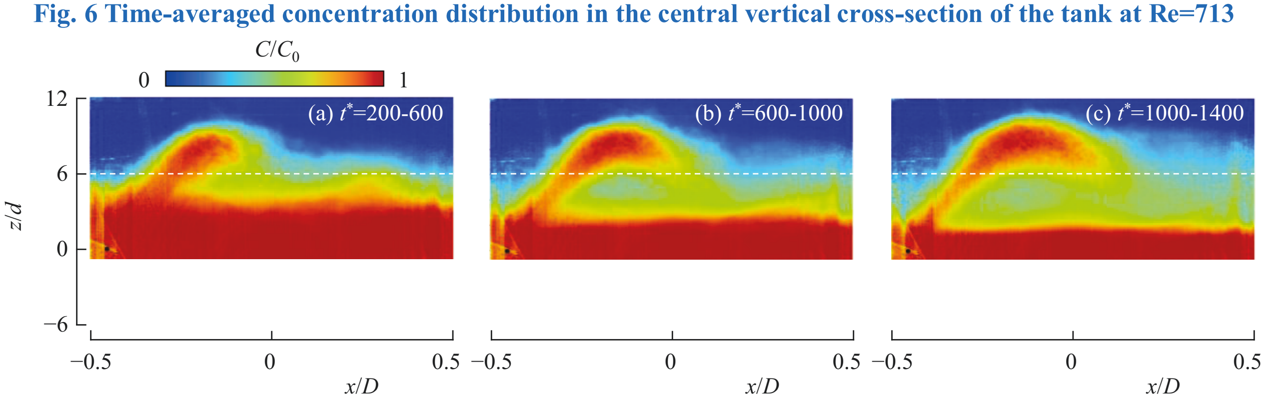

Fig. 7 Time-averaged concentration distribution in the central vertical cross-section of the tank at Re=2139

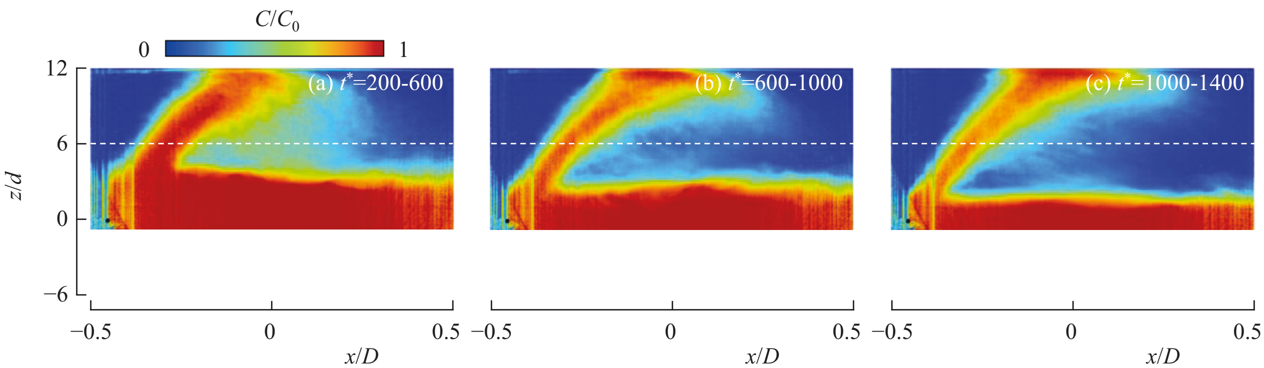

Fig. 8 Time-averaged concentration distribution in the central vertical cross-section of the tank at Re=3565

3.3 Progress of Mixing

To estimate the progress of the mixing in the tank, a root-mean-square of the concentration C, namely C_{rms}, is calculated in the central vertical cross-section by the following equation:

$$C_{\mathrm{rms}} = \sqrt{\frac{1}{N}\sum_{i}^{N}(C_i - \bar{C})^2}$$

where C_i is the value of C at pixel i, N is the number of measuring points, i.e. a number of pixels in the measured area, and $\overline{C}$ is the mean value of C in the measured area. The value of C_{rms} decreases during the course of mixing. In this study, C_{rms} is calculated in the range of $-0.405 \leq x/D \leq 0.405$ and $0 \leq z/d \leq 12$, as shown in Fig. 9, to exclude noises near the edges of image because of the shape of the tank. Fig. 10 shows the temporal evolution of C_{rms} in the central vertical cross-section passing through the nozzle centerline ($y = 0$). When Re=713 (Pattern A), C_{rms} decreases in the constant and relatively gentle gradient with the lapse of time. Because the weak mixing is generated by the horizontal flow along the density interface, C_{rms} decreases slowly. When Re=2139 (Pattern B), C_{rms} also decreases in the constant gradient with the lapse of time. Mixing proceeds by diffusion of the lower fluid in the upper layer and by the heaving of interface caused by the downward flow, while thickness of the intermediate density layer increases. When Re=3565 (Pattern C), C_{rms} declines markedly at $t^* < 200$. Under this condition, mixing generated by the heaving of interface becomes weak because the lower fluid transported by the jet widely and horizontally spreads in the upper layer. The marked decline of C_{rms} at $t^* < 200$ is attributable to sudden and transient fluid motion owing to issuing of the jet into the quiescent fluids. However, the time rate of change in C_{rms} becomes less at $t^* \geq 200$. During this period, mixing proceeds by the diffusion of the lower fluid in the upper layer after the transient fluid motion has been settled.

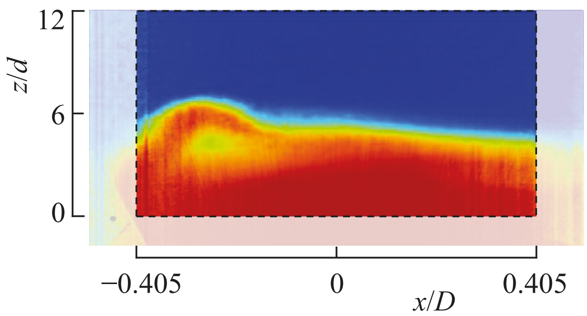

Fig. 9 Evaluation area for root-mean-square of concentration, C_{rms}

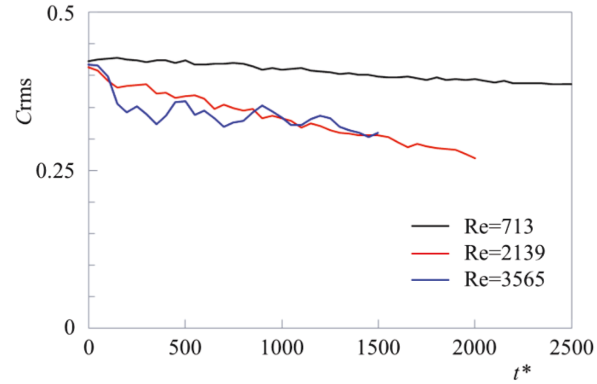

Fig. 10 Time evolution of C_{rms} in the central vertical cross-section of the tank

3 Summary

In this study, quantitative investigations of mixing phenomena by a jet issuing into a two-layer density-stratified fluid in a cylindrical tank have been conducted. The velocity and concentration fields in the central cross-section passing through the jet centerline were measured using PIV and PLIF, respectively. The experiments clarified the relations between the jet behavior and mixing phenomena.

At Re=713, in the case that the jet reaches the interface without penetrating it, the jet pushes the interface up locally and then spreads almost horizontally along the interface. The mixing gently proceeds near the interface because of the horizontal flow just below the interface.

At Re=2139, in the case that the jet penetrates the interface but does not reach the upper water surface, the mixing is mainly generated by the heaving of interface caused by the horizontal flow owing to the collision between the jet and the density interface.

At Re=3565, in the case that the jet reaches the upper water surface, the mixing proceeds due to the diffusion of lower fluid, which is transported by the jet, in the upper layer.

The mixing proceeds actively as the Reynolds number increases. However, the progress of mixing at Re=3565, corresponding to the gradient in the decrement of the root-mean-square of the concentration, becomes almost the same as that at Re=2139 after the transient fluid motion has been settled.

References

[1] Baines WD, Turner JS and Campbell IH. Turbulent fountains in an open chamber. *Journal of Fluid Mechanics*, Vol.212, pp.557-592, 1990.

[2] Bloomfield LJ and Kerr RC. Turbulent fountains in a stratified fluid. *Journal of Fluid Mechanics*,Vol.358, pp.335-356, 1998.

[3] Lin YJP and Linden PF. The entrainment due to a turbulent fountain at a density interface. *Journal of Fluid Mechanics*, Vol.542, pp.25-52, 2005.

[4] Ansong JK, Kyba PJ and Sutherland BR. Fountains impinging upon a density interface. *Journal of Fluid Mechanics*, Vol.595, pp.115-139, 2008.

[5] Shakouchi S, Fukue S and Uchiyama T. Investigation of the behavior of a jet issued into two-layer density-stratified fluid. *Journal of Flow Control, Measurement and Visualization*, Vol. 3, No. 1, pp. 1-9, 2015.

[6] Degawa T, Fukue S, Uchiyama T, Ishikawa A and Motoyama K. Behavior of a jet issuing diagonally upward into two-layer density-stratified fluid in a cylindrical tank. *Journal of Flow Control, Measurement and Visualization*, Vol. 5, No. 3, pp. 51-64 2017.

[7] Shakouchi S, Shimada S and Uchiyama T. Numerical simulation of jet flow issued into density-stratified fluid by Vortex in Cell method. *Advances and Applications in Fluid Mechanics*, Vol. 17, pp. 115-134, 2015.

[8] Degawa T, Uchiyama T, Aozasa I, Ishikawa A and Motoyama K. Numerical simulation of jet issuing diagonally upward into density-stratified fluid in cylindrical tank. *Journal of Power and Energy Engineering*, Vol. 6, No. 3, pp. 38-52, 2018.

[9] Suzuki H, Nagata K and Sakai Y. Quantitative visualization of high-Schmidt-number turbulent mixing in grid turbulence by means of PLIF. *Journal of Visualization*, Vol. 15, No. 2, pp. 109-117, 2012.

Copyright Statement